Research Square

Preprints are preliminary reports that have not undergone peer review.
They should not be considered conclusive, used to inform clinical practice,
or referenced by the media as validated information.

Isolation and identification of nitrate reducing microbial induced carbonate precipitation bacteria and treatment of synthetic tannery wastewater

Bhanu Pratap Singh

bhanu.2022rce04@mnnit.ac.in

MNNIT Allahabad: Motilal Nehru National Institute of Technology https://orcid.org/0009-0000-5152-9439

Dr. Debolina Basu

MNNIT Allahabd: Motilal Nehru National Institute of Technology

Dr. Joyabrata mal

MNNIT: Motilal Nehru National Institute of Technology

Research Article

Keywords: Nitrate-reducing pathway, Microbial induced carbonate precipitation, Hexavalent chromium, Bacillus pumilus

Posted Date: November 16th, 2026

DOI: https://doi.org/10.21203/rs.3.rs-11719257/v1

License: This work is licensed under a Creative Commons Attribution 4.0 International License.
Read Full License

Additional Declarations: The authors declare potential competing interests as follows: -

Abstract:

Microbial-induced carbonate precipitation is a technique used for the heavy metal removal process, but the nitrate removal pathway was rarely used. The hexavalent chromium-resistant *Bacillus pumilus* was isolated and used to treat synthetic tannery wastewater. In this treatment process, the maximum removal efficiency in 15 mg/L hexavalent chromium-containing synthetic tannery wastewater was COD 94.241%, NO_3^- 97.783%, Cr(VI) 49.254%, and pH increased from 7.04 to 8.49 in zero-day to 28th day. Moreover, the nitrate-reducing activity of *Bacillus pumilus* in the experiment was identified by the conversion of $NO_3 - N$ to $NO_2 - N$, which was identified by a nitrite-detecting colour reagent process. The XRD analysis identified the different mineral compositions of magnesian calcite ($CCa_{0.9}Mg_{0.1}O_3$), calcium chromate ($CaCrO_4$), chromic oxide (Cr_2O_3), and chromium dioxide (CrO_2). Overall, the combination of *Bacillus pumilus* and nitrate-reducing MICP technology is an environmentally friendly strategy.

Keywords: Nitrate-reducing pathway, Microbial induced carbonate precipitation, Hexavalent chromium, *Bacillus pumilus*.

Introduction:

The population is continuously increasing, which increases demand for high-quality industrial products. In industrial production, wastewater originates from the manufacturing of the products. In India, tannery industrial effluent is ranked highest in pollution among all industries. These industries, in particular, contribute to hexavalent chromium pollution (Abdulmalik et al., 2023). In the tannery industry, the physical and chemical processes are important to convert rawhide into salable leather that impart stability and good market quality (Sawalha et al., 2019). The animal skin is removed during the leather manufacturing process and forms waste products, including dead cells, carbohydrates, proteins, fat, minerals, and

muscle tissue (Sawalha et al., 2019). 70% of the total pollutants were formed by TDS, BOD, and COD, produced by the soaking, liming, degreasing, and tanning processes (Islam et al., 2014). Pollutants from the tannery industry have been characterised as high salinity levels, turbidity, solids, chromium, colour, and nitrogen. These pollutants are directly discharged into the water body without proper treatment (Ramírez et al., 2019). According to the World Health Organization (WHO), water pollution is the main public health problem (Georgaki & Charalambous, 2023).

Hexavalent chromium demand is increasing steadily due to its extensive use across various industries and chemical processes. These industrial wastewater samples contained 10-100 mg/L of chromium, and hexavalent chromium is a highly toxic pollutant at low concentrations (Kabir et al., 2018). Chromium concentrations above 6 mg/L affected human health. It causes oral fungal infections, reduced blood sugar, ulcers, hyposalivation, dermatitis, irritation, corrosive reactions in the nasal septum, pharynx cancers, and hyperglycemia-increased urinary excretion (Karri et al., 2021). Chromium has received significant attention as a wastewater pollutant, so the biological nitrogen removal process was used to treat this toxic pollutant. In the biological denitrification process, Cr(VI) enters the bacterial cytoplasmic matrix and reduced to Cr(III) (Niu et al., 2025). The biological denitrification pathway is a challenge for treatment.

Existing research has focused on the treatment of metal removal from wastewater using denitrification and nitrification in the microbial-induced carbonate precipitation process. The denitrifying strain *Pseudomonas sp.* produced the microbial-induced carbonate precipitation. In this process, the initial concentrations of Cd(II) 3.00 mg/L, Ca(II) 180.00 mg/L, and NO_3^-– N 16.50 mg/L were identified in the heterotrophic medium (HM).

After the treatment, *Pseudomonas sp.* removed Cd(II), Ca(II), and NO_3^-– N (Wang et al., 2024). Jiaran Liu et al., in 2022, used the Yulong filler biofilm reactor; this reactor was operated under anaerobic conditions. This denitrifying strain *Cupriavidus sp.* was used in this reactor for the treatment of heterotrophic medium, and after the treatment, NO_3^-– N, Ca^{2+}, and F^- were removed (Liu et al., 2022a). The *Acinetobacter* sp. H12 was removed Ni^{2+}, Ca^{2+}, and produced $Ca_5(PO_4)_3OH$, $NiCO_3$, and $CaCO_3$ in an immobilized biofilm reactor (Liu et al., 2021). Marwa Eltarahony conducted a lab-scale study in 2020 to remove lead and mercury using the denitrification pathway with *Proteus mirabilis*. The X-ray diffraction identified the calcite as $PbCO_3$, Pb_2O, $CaPbO_3$, Hg, and Hg_2O (Eltarahony et al., 2020). In a lab-scale study, it was identified that *Ochrobactrum sp.* was capable of biomineralisation, denitrification, and heavy-metal removal. In this biomineralisation, precipitated samples were identified as $CaCO_3$, $ZnCO_3$, and $Cd_5(PO_4)_3OH$ (Li et al., 2022).

Therefore, an anaerobic denitrification microbial-induced carbonate precipitation pathway was used to treat pollutants. The main objectives of this work, (i) to isolate a nitrate-reducing bacteria under anaerobic conditions with the help of a nitrate-reducing medium, and to identify this bacterium. (ii) This bacteria was used for the treatment of the synthetic tannery wastewater, with different chromium concentrations. The different physicochemical characteristics were identified in the precipitated sample after the treatment of synthetic tannery wastewater and before treatment.

2. Materials and Methods:

2.1. Source, enrichment, and isolation:

In this experiment, a sludge sample was collected from the sewage treatment plant (STP) Rajapur, Prayagraj, Uttar Pradesh, India. The 100 mL serum bottle was filled with the 2 gm

sludge sample, which was closed with a butyl rubber stopper and crimped. The syringe was used to transfer 90 mL of modified nitrate-reducing Clark medium: Peptone 20.0 gm/L, KNO_3 2.0 gm/L, $Ca(NO_3)_2.4H_2O$ 2.0 gm/L, and amended with 100 mg/L hexavalent chromium stock solution. After this, the serum bottle was purged with N_2 for 10 minutes. This bottle was incubated at a temperature of 35˚C without shaking for 28 days. After enrichment, the nitrate-reducing pure culture was isolated on nitrate-reducing agar Clark medium (Atlas, 2010).

The pure cultures' nitrate-reducing activity was assessed qualitatively to determine the reduction of nitrate to nitrite by nitrate-reducing bacteria. The different pure cultures were isolated overnight in nitrate-reducing Clark broth. Nitrite detection was calculated by adding a nitrite-detecting colour reagent. The nitrite-detecting colour reagent was prepared by mixing N-(1-naphthyl) ethylenediamine dihydrochloride 1 gm/L, sulfanilamide 10 gm/L, and 85% phosphoric acid 100 mL/L. The 2×10^{-1} mL colour reagent was added to 5 mL of overnight culture Clark broth sample. After 10 min, the sample colour stabilised and identified at an optical density of 543 nm using a UV-Vis spectrophotometer. The measured nitrite-N produced by the degradation of nitrate-N, along with the degradation efficiency, was evaluated (Subedi et al., 2017). The nitrate-to-nitrite reducing pure culture NR20 identification was obtained by PCR amplification of DNA corresponding to 16S rRNA primes F27 (5′-AGAGTTTGATCCTGGCTCAG-3′) and R1492 (5′-CTACGGCTACCTTGTTACGA-3′) were used to amplify the 16S rRNA gene of strain NR20 (Kolbert & Persing, 1999).

2.2. Synthetic tannery wastewater treatment:

The performance of simultaneous COD, NO_3^-– N, and Cr(VI) removal was evaluated following treatment of synthetic tannery wastewater. The wastewater was treated in a 100 mL serum bottle sealed with a butyl rubber stopper, crimped, and purged with N_2 for 10 minutes.

This synthetic tannery wastewater was inoculated with the nitrate-reducing strain NR20. The different experimental sample replicates of synthetic tannery wastewater were prepared with varying concentrations of Cr(VI) stock solution and incubated at 35˚C. (a) Case-1: 89 mL synthetic tannery wastewater contained hexavalent chromium, with concentrations of 100 mg/l, 75 mg/l, 50 mg/l, 25 mg/l, 20 mg/l, and 15 mg/l, and inoculated with 1 mL sulfate-reducing pure culture. (b) Case-2: 89 mL synthetic tannery wastewater without hexavalent chromium and incubated with 1 mL sulfate-reducing pure culture. The different chemical composition of the synthetic tannery wastewater: Starch ($C_6H_{10}O_5$) 6000 mg/L, Urea (CH_4N_2O) 900 mg/L, Zinc sulfate heptahydrate ($ZnSO_4.7H_2O$) 0.12 mg/L, Ammonium chloride (NH_4Cl) 133.7 mg/L, Sodium chloride (NaCl) 330.0 mg/L, Sodium bicarbonate ($NaHCO_3$) 336.0 mg/L, Manganese sulfate monohydrate ($MnSO_4.H_2O$) 28.0 mg/L, Disodium phosphate (Na_2HPO_4) 275.0 mg/L, Magnesium sulfate heptahydrate ($MgSO_4.7H_2O$) 200 mg/L, Ferric chloride hexahydrate ($FeCl_3.6H_2O$) 1.0 mg/L, Calcium sulfate dihydrate ($CaSO_4.2H_2O$) 5 mg/L, Calcium chloride ($CaCl_2$) 15.0 mg/L, Potassium nitrate (KNO_3) 252.5 mg/L, pH was maintained 7±.5 of synthetic tannery wastewater (Jia et al., 2018; Latkar & Chakrabarti, 1994; Lay, 2000). The synthetic tannery wastewater COD, NO_3^-– N, Cr(VI) concentration, and pH were measured at 0, 7, 14, 21, and 28 days (Abi et al., 2018; Algaifi et al., 2020; Bidu et al., 2023; Elmelouky et al., 2018; Pawlak & Pawlak, 1999; Varghese et al., 2023; Wu & Cao, 2013; Zhou & Boyd, 2016).

3. Results:

3.1. Isolation and Identification:

After anaerobic enrichment of the nitrate-reducing bacteria, the pure culture was isolated on agar media. The selection of a nitrate-reducing pure culture is done by growing the culture in nitrate-reducing Clark broth medium. In the broth medium pure culture sample, the nitrite-detecting colour reagent was added, which changed the medium colour, showing nitrate (NO_3^-

) reduction to nitrite (NO_2^-) (Figure 2). Strain NR20 showed nitrate-reducing activity; therefore, the BLAST result showed the highest similarity with that of Bacillus pumilus. The neighbour-joining phylogenetic tree was constructed from the 16S rRNA gene sequences of the isolate and other phylogenetically related strains (Figure 1) (Fang et al., 2024).

3.2. Synthetic tannery wastewater characterization:

The synthetic tannery wastewater (STW) contained the NO_3^- 302 ± 5.945 mg/L, COD 884.323 ± 235.165 mg/L and NH_4 – N 560.932 ± 63.73 mg/L, and Cr(VI) concentration of 15 mg/L - 100 mg/L Cr(VI). This Cr(VI) tolerant bacterial community had the ability to remove the COD concentration from the synthetic tannery wastewater. In Figure 3 (a) & Table 1. shows a 15 mg/L hexavalent chromium-containing synthetic tannery wastewater; the COD removal efficiency was 81.395 ± 1.437% to 92.043 ± 2.198% from 7^{th} days to 28^{th} days, respectively, and in the 100 mg/L hexavalent chromium contained synthetic tannery wastewater COD removal rate 71.183 ± 4.472% to 77.745 ± 2.654% from 7^{th} days to 28^{th} days, respectively. The COD degradation was identified in the anaerobic biological treatment setup of serum bottles (Fazal et al., 2019). The COD parameter indicates the magnitude of contamination in the wastewater; the COD concentration was dependent upon the organic matter in the synthetic tannery wastewater, which was degraded by the nitrate-reducing microorganisms (Reyes-Romero et al., 2021). In this treatment process, the COD concentration decreased due to different enzymes. Bacillus sp. had an important role in decomposing cellulose and lipids. Lipids were degraded into fatty acids and glycerol, which were used as a source of nutrients by microbes. Starch is a polysaccharide that is built by a glycosidic bond, which was decomposed by Bacillus sp., and worked as an organic nutrient in synthetic tannery wastewater. Bacillus pumilus produced high amount of cellulase enzymes, So these Bacillus pumilus strongly

supports synthetic tannery wastewater treatment. The organic matter of the synthetic tannery wastewater was broken down, and formed the reduction of COD. Therefore, the COD concentration was decreased by the consortium of Bacillus pumilus (Priadie et al., 2014).

Insert Table 1

An experiment on Cr(VI) removal in synthetic tannery wastewater was conducted with different concentrations of Cr(VI). Figure 3 (b) & Table 2. the 15 mg/L hexavalent chromium contained synthetic tannery wastewater removed the 40.176 ± 1.964% to 48.137 ± 1.117% from the 7^{th} day to the 28^{th} day, respectively. The 100 mg/L Cr(VI) containing synthetic tannery wastewater, showed Cr(VI) removal of 17.269 ± 1.072% to 23.228 ± 2.671% from the 7^{th} day to the 28^{th} day, respectively. In the hexavalent chromium removal process, carbon sources are required, which facilitate the removal of chromium through microbial activity. The time taken also depended on the removal of the initial chromium concentration. In the serum bottle, the chromate removal required metabolically active microorganisms along with the carbon sources. Bacillus pumilus worked as electron donors and released Cr(VI) reducing agents from the extracellular polymeric substances matrix. In this batch experiment, denitrification of nitrate and Cr(VI) occurred simultaneously (Reddy & Nancharaiah, 2018).

Insert Table 2

In Figure 3 (c) & Table 3. the NO_3^-(nitrate) removal efficiency increased from 15 mg/L of Cr(VI) containing synthetic tannery wastewater. NO_3^-(nitrate) removed 25.865 ± 2.653% to 95.794 ± 1.989% from 7th day to 28th day, respectively. In the 100 mg/L Cr(VI) containing synthetic tannery wastewater, the Cr(VI) was removed 3.825 ± 2.491% to 88.106 ± 3.196% from 7th day to 28th day, respectively. The rate-limiting steps of the MICP denitrification process involve the oxidation of the C-sources by the nitrate-reducing bacteria (Eq.(2)) and the $CaCO_3$ crystals around the cells (Erşan et al., 2015a).

Insert Table 3

Figure 3 (d) & Table 4. the 15 mg/L Cr(VI) contained synthetic tannery wastewater increased the pH value 7±0.04 to 8.41±0.08 from zero day to the 28th day, respectively. The pH of 100 mg/L Cr(VI) containing synthetic tannery wastewater increased 7 ± 0.05 to 8.41±0.08 from zero day to the 28th day, respectively. In this denitrification process, the pH value continuously increased from zero days to 28 days during the experiment. The gradual conversion of the alkaline aqueous environment facilitated the hydration of CO_2 to form CO_3^{2-}. This condition formed a supersaturated environment and enhanced the accumulation of bio-crystalline particles, which led to precipitation. In this anaerobic condition, the pH value continuously increases and forms the MICP. In this experiment, Cr(VI), Ca^{2+}, and NO_3^-– N were constantly removed with respect to the days (Liu et al., 2022a; Yang et al., 2022).

199 ----------

200 Insert Table 4

201 ----------

202 ----------

203 Insert Figure 3

204 ----------

205

206 **3.1. FT-IR analysis:**

207

208 In this nitrate-reducing MICP process, the pure culture played an important role. In this
209 biomeneralization experiment, the different functional groups were identified. The ATR PRO
210 4X + FT/IR-4X was used for the identification of the functional groups. The two samples were
211 identified as (a) Case-1: Synthetic tannery wastewater with Cr(VI) concentration, and (b) Case-
212 2: Synthetic tannery wastewater without Cr(VI) concentration. Figure 4, shows the different
213 infrared characteristic peaks in the range of 400 – 4000 cm^{-1}. The −N–H (Aliphatic primary
214 amine) functional group ranges from 3500 – 3300 cm^{-1}. In case-2 wastewater, the peaks at
215 3407.6 cm^{-1}, 3462.56 cm^{-1}, and case-1 wastewater show the −N–H (Aliphatic primary amine)
216 functional group (Negm et al., 2018). In case-2 wastewater sample, the peaks at 3407.6 cm^{-1},
217 3462.56 cm^{-1}, and in case-1 wastewater, the peaks at 3423.03 cm^{-1}, 3407.6 cm^{-1}, these peaks
218 show the −N–H (Aliphatic primary amine) functional group (Negm et al., 2018). The – OH
219 (alcohol) bond groups show the plane-bending range between the 3400 – 3700 cm^{-1}. The –
220 OH (alcohol) functional groups showed 3665.05 cm^{-1}, 3598.51 cm^{-1} in the case-2 wastewater
221 sample, and the Cr(VI) containing wastewater sample showed 3507.88 cm^{-1}, 3598.52 cm^{-1}.

The C-H (Alkyne) functional group is considered to be 2800 − 3000 cm^{-1}. The case-1 wastewater sample showed the C-H (Alkyne) functional group at 2945.73 cm^{-1}, 2862.81 cm^{-1} and the case-2 wastewater sample showed 2862.81 cm^{-1}, 2945.73 cm^{-1} and these groups represent the cell wall components, cell membrane, nucleic acids, and cellular proteins. The C=O group represents the range between the 1700 − 2000 cm^{-1}. The case-2 wastewater sample shows 1714.41 cm^{-1}, and 1710.55 cm^{-1} the case-1 wastewater sample. The C-O functional group is represented between the wavenumbers of 600 −1000 cm^{-1}. This C-O functional group represents $CaCO_3$, in the case-2 wastewater sample shown the wave number of 760.78 cm^{-1}, 829.241 cm^{-1}, 871.667 cm^{-1}, 829.241 cm^{-1}, 986.411 cm^{-1}, and in the case-1 wastewater sample shown the wavenumber of 999.91 cm^{-1}, 829.241 cm^{-1} (Esmail et al., 2022). The carbonate ion (CO_3^{2-}) shown the vibratio range from 1392 cm^{-1} – 1476 cm^{-1}. In the case-2 wastewater sample shown the 1418.39 cm^{-1}, 1455.52 cm^{-1} and in the Cr(VI) contain case-1 sample shown the wavenumber of 1455.99 cm^{-1}. These all wavenumber represents the presence of $CaCO_3$ in the mineralized sample (Acikgoz et al., 2021). The nitrate (NO_3^-) functional group represents the wavenumber between the 1630 −1613 cm^{-1}. In the case-2 wastewater sample shown, the wavenumber 1626.85 cm^{-1}, and in the Cr(VI) containing case-1 wastewater sample shown, the 1624.04 cm^{-1} (Çayirtepe, 2004).

Insert Figure 4

3.2. XRD analysis:

In Figure 5, the X-ray Diffraction (Rigaku, Model-Smart lab 3kW) was used for nitrate reducing micp samples analysis. The XRD data confirmed that $CaCO_3$ was present in case-1 & case-2. The XRD $CaCO_3$ data of all minerals were similar to the $CaCO_3$ JCPDS 05-0586 data (Wang et al., 2021). The magnesian calcite ($CCa_{0.9}Mg_{0.1}O_3$) was produced in both case-1 & case-2, which had bond length values of $\boldsymbol{a}$ = 4.9410 A˚ and $\boldsymbol{c}$ = 16.8540 A˚. This value was larger than the bond values $\boldsymbol{a}$ = 4.8033 A˚ and $\boldsymbol{c}$ = 15.984 A˚ of the magnesian calcite ($CaMg(CO_3)_2$) (Althoff., 1977). In this treatment experiment, the $CaCrO_4$ was precipitated in the form of Cr(VI), and Cr_2O_3 and CrO_2 were also precipitated in the form of Cr(III) and Cr(IV), respectively.

Insert Figure 5

Discussion:

In this experiment, the nitrate-reducing microbial-induced carbonate precipitation process is the main focus of the wastewater treatment process. The heterotrophic nitrifying strains can produce HNAD (Heterotrophic nitrification-aerobic denitrification). This produces Ca^{2+} precipitation, removes NH^{4+}-N, and precipitates micp during synthetic tannery wastewater treatment (Li et al., 2024). The denitrification-micp process is the dominant process in the presence of organic carbon and nitrate (NO_3^-) under limited conditions. This is represented by a highly negative standard Gibbs free energy (ΔG˚) (Eq. (1)). In the biological reduction process, these ions NO_3^-, CO_3^{2-}, and HCO_3^- are necessary ions for $CaCO_3$ precipitation (Erşan et al., 2015b).

$$CH_2COO^- + 2.6H^+ + 1.6NO_3^- \rightarrow 2CO_2 + 0.8N_2 + 2.8H_2O$$

$$G^\circ = -785\ KJ/mol \quad (1)$$

In the denitrification MICP process, denitrifying microbes, especially abundant in polluted areas, landfills, and eutrophic lakes, are beneficial to the environment by removing nitrogen via denitrification. The organic matter denitrifies nitrate and generates alkalinity, carbon dioxide, and nitrogen gas. Carbon dioxide equilibrates with water to form bicarbonate ions. In an alkaline environment, bicarbonate ions, divalent cations, and hydroxide ions precipitate the carbonate biomineral. The different denitrification processes are shown in the equations (Equations 2 – 4) (Bu et al., 2022; Jain et al., 2021; Wang et al., 2023).

$$(CH_3COOH)_2 + NO_3^- \rightarrow \frac{4}{5}N_2 + 3CO_2 + 3H_2O + OH^- \quad (2)$$

$$3CO_2 + 3H_2O \rightarrow HCO_3^- + H^+ \quad (3)$$

$$M^{2+} + HCO_3^- + OH^- \rightarrow MCO_3 + H_2O \quad (4)$$

Conclusion:

In this study, the nitrate-reducing strain *Bacillus pumilus* mineralized the Cr(VI) in the synthetic tannery wastewater and precipitated the calcite. This synthetic tannery wastewater contained COD 819.240 mg/L, NO_3^-307.945 mg/L, and Cr(VI), 15 - 100 mg/L. In this study, the 15 mg/L Cr(VI) containing synthetic tannery wastewater removed 40.176±1.964% on the 28th day. The maximum COD concentration was removed 92.043 ± 2.198% on the 28th day. The 15 mg/L Cr(VI) contained STW sample removed the NO_3^-(nitrate) of 95.794 ± 1.989% on 28th day. In the nitrate removal process, the nitrite produced in the 15 mg/L Cr(VI) contained STW sample was 29.683 ± 1.376% to 79.805 ± 1.395% from the 7th day to the 28th day. In this pathway, the pH value increased from 7±0.04 to 8.41±0.08 from zero to the 28th day, respectively. The nitrate (NO_3^-) functional group represents the wavenumber between the 1630

295 −1613 cm^{-1}. In the synthetic tannery wastewater without Cr(VI) sample, the wavenumber
296 1626.85 cm^{-1}, and in the Cr(VI) containing synthetic tannery wastewater sample shown, the
297 1624.04 cm^{-1}. The carbonate ion (CO_3^{2-}) shown the vibratio range from 1392 cm^{-1} – 1476
298 cm^{-1}. In the synthetic tannery wastewater without Cr(VI) sample shown the 1418.39 cm^{-1},
299 1455.52 cm^{-1}, and in the Cr(VI) containing synthetic tannery wastewater sample shown the
300 wavenumber of 1455.99 cm^{-1}. All these wave numbers present the presence of $CaCO_3$ in the
301 mineralized synthetic tannery wastewater sample. The XRD data confirmed that the $CaCO_3$
302 mineral was present in the synthetic tannery wastewater without Cr(VI) sample, and Cr(VI)
303 contained a sample. The XRD $CaCO_3$ data of all minerals were similar to the $CaCO_3$ (JCPDS
304 05-0586) data. The magnesian calcite ($CCa_{0.9}Mg_{0.1}O_3$) was produced in both the without
305 Cr(VI) synthetic tannery wastewater sample and chromium-containing synthetic tannery
306 wastewater samples, which had bond length values of ***a*** = 4.9410 A˚ and ***c*** = 16.8540 A˚. This
307 value was larger than the bond value ***a*** = 4.8033 A˚ and ***c*** = 15.984 A˚ of the magnesian calcite
308 ($CaMg(CO_3)_2$).
309
310 **CrediT authorship contribution statement:**
311 **Bhanu Pratap Singh:** Writing – organization draft, Conceptualization, Methodology, Data
312 curation. **Debolina Basu:** Supervision, Formal analysis, Investigation. **Joyabrata Mal:**
313 Supervision, Formal analysis, Investigation.
314 **Declaration of competing interests:**
315 The authors declare that they have no known competing financial interests or personal
316 relationships that could have appeared to influence the work reported in this paper.
317 **Acknowledgments:**

This work was supported by the Department of Civil Engineering, Department of Biotechnology, Motilal Nehru National Institute of Technology, Allahabad, Prayagraj, U. P. (211004), India.

Reference:

1. Acikgoz, A., Ceyhan, G., Aktas, B., Yalcin, S. and Demircan, G., 2021. Luminescent, structural and mechanical properties of erbium oxide doped natural obsidian glasses. Journal of Non-Crystalline Solids, 572, 121104. 10.1016/j.jnoncrysol.2021.121104
2. Eltarahony, M., Zaki, S. and Abd-El-Haleem, D., 2020. Aerobic and anaerobic removal of lead and mercury via calcium carbonate precipitation mediated by statistically optimized nitrate reductases. Scientific reports, 10(1), 4029. https://doi.org/10.1038/s41598-020-60951-1
3. Abdulmalik, A.F., Yakasai, H.M., Usman, S., Muhammad, J.B., Jagaba, A.H., Ibrahim, S., Babandi, A. and Shukor, M.Y., 2023. Characterization and invitro toxicity assay of bio-reduced hexavalent chromium by Acinetobacter sp. isolated from tannery effluent. Case Studies in Chemical and Environmental Engineering, 8, 100459. https://doi.org/10.1016/j.cscee.2023.100459
4. Atlas, R.M., 2010. Handbook of microbiological media.
5. Çayırtepe, İ., 2004. Ft-ir Spectroscopic Characterization of the Intermediates in the Selective Catalytic Reduction of no With Methane on Pd/zro2-wox Catalyst (Master's thesis, Bilkent Universitesi (Turkey)). https://search.proquest.com/openview/1a52ddcc7fb4f094c91052173e927f71/1?pq-origsite=gscholar&cbl=2026366&diss=y
6. Algaifi, H.A., Bakar, S.A., Sam, A.R.M., Ismail, M., Abidin, A.R.Z., Shahir, S. and Altowayti, W.A.H., 2020. Insight into the role of microbial calcium carbonate and the factors involved in self-healing concrete. Construction and Building Materials, 254, 119258. https://doi.org/10.1016/j.conbuildmat.2020.119258
7. Esmail, R., Afshar, A., Morteza, M., Abolfazl, A. and Akhondi, E., 2022. Synthesis of silver nanoparticles with high efficiency and stability by culture supernatant of Bacillus ROM6 isolated from Zarshouran gold mine and evaluating its antibacterial effects. BMC microbiology, 22(1), 97. https://doi.org/10.1186/s12866-022-02490-5
8. Bu, C., Lu, X., Zhu, D., Liu, L., Sun, Y., Wu, Q., Zhang, W. and Wei, Q., 2022. Soil improvement by microbially induced calcite precipitation (MICP): a review about mineralization mechanism, factors, and soil properties. Arabian Journal of Geosciences, 15(9), 863. https://doi.org/10.1007/s12517-022-10012-w
9. Erşan, Y.Ç., De Belie, N. and Boon, N., 2015b. Microbially induced $CaCO_3$ precipitation through denitrification: an optimization study in minimal nutrient environment. Biochemical Engineering Journal, 101, 108-118. http://dx.doi.org/10.1016/j.bej.2015.05.006
10. Elmelouky, A., Mortadi, A., Chahid, E. and Elmoznine, R., 2018. Impedance spectroscopy as a tool to monitor the adsorption and removal of nitrate ions from aqueous solution using zinc aluminum chloride anionic clay. Heliyon, 4(2). https://doi.org/10.1016/j.heliyon.2018

11. Erşan, Y.Ç., De Belie, N. and Boon, N., 2015a. Microbially induced $CaCO_3$ precipitation through denitrification: an optimization study in minimal nutrient environment. Biochemical Engineering Journal, 101, 108-118. http://dx.doi.org/10.1016/j.bej.2015.05.006
12. Fazal, S., Xu, H., Xu, X., Huang, S., Zhang, Y., Ali, A., Hayat, W., You, Y., Du, X. and Ullah, Z., 2019. Simultaneous removal of carbon, sulfur, and nitrogen from biological synthetic wastewater: aerobic and anaerobic approach. Arabian Journal of Geosciences, 12(5), 168. https://doi.org/10.1007/s12517-019-4346-8
13. Fang, C. and Achal, V., 2024. Enhanced steel corrosion inhibition through microbially induced carbonate precipitation with facultative anaerobic denitrifying bacterium. Case Studies in Construction Materials, 21, 03607. https://doi.org/10.1016/j.cscm.2024.e03607
14. Kiran Kumar Reddy, G. and Nancharaiah, Y.V., 2018. Sustainable bioreduction of toxic levels of chromate in a denitrifying granular sludge reactor. Environmental Science and Pollution Research, 25(2), 1969-1979. https://doi.org/10.1007/s11356-017-0600-3
15. Georgaki, M.N. and Charalambous, M., 2023. Toxic chromium in water and the effects on the human body: a systematic review. Journal of Water and Health, 21(2), 205-223. https://doi.org/10.2166/wh.2022.214
16. Islam, B.I., Musa, A.E., Ibrahim, E.H., Sharafa, S.A. and Elfaki, B.M., 2014. Evaluation and characterization of tannery wastewater. Journal of Forest Products & Industries, 3(3), 141-150.
17. Jia, H., Liu, W., Wang, J., Ngo, H.H., Guo, W. and Zhang, H., 2018. Optimization of sensing performance in an integrated dual sensors system combining microbial fuel cells and upflow anaerobic sludge bed reactor. Chemosphere, 210, 931-940. https://doi.org/10.1016/j.chemosphere.2018.07.119
18. Melesse, A.G., Srinivasan, S.V., Demissie, B.A. and Chacko, S.P., 2020. Sequencing batch airlift reactor system for simultaneous removal of nitrogen and organic carbon from synthetic tannery wastewater. Desalination and Water Treatment, 183, 194-204. https://doi.org/10.5004/dwt.2020.25029
19. Jain, S., Fang, C. and Achal, V., 2021. A critical review on microbial carbonate precipitation via denitrification process in building materials. Bioengineered, 12(1), 7529-7551. https://doi.org/10.1080/21655979.2021.1979862
20. Kabir, M.M., Fakhruddin, A.N.M., Chowdhury, M.A.Z., Pramanik, M.K. and Fardous, Z., 2018. Isolation and characterization of chromium (VI)-reducing bacteria from tannery effluents and solid wastes. World Journal of Microbiology and Biotechnology, 34(9), 126. https://doi.org/10.1007/s11274-018-2510-z
21. Karri, R.R., Ravindran, G. and Dehghani, M.H., 2021. Wastewater sources, toxicity, and their consequences to human health. In Soft computing techniques in solid waste and wastewater management, 3-33. http://dx.doi.org/10.1016/B978-0-12-824463-0.00001-X
22. Priadie, B., Rinjani, R.R., Arifin, Z.M., Safitri, R. and Imanda, N., 2014. Bioremediation of Cimuka River stream by the consortium of Bacillus coagulans, Bacillus pumilus, Bacillus subtilis, Paenibacillus amyloliticus, and Nitromonas sp. Scientific Papers. III: Series E. Land Reclamation. Earth Observation & Surveying, Environmental Engineering. https://landreclamationjournal.usamv.ro/pdf/2014/Art5.pdf
23. Niu, H., Wang, C., Luo, X., Li, P., Qiu, H., Jiang, L., Maimaitiaili, S., Wu, M., Xu, F. and Xu, H., 2025. Cr (VI) reduction, electricity production, and microbial resistance

variation in paddy soil under microbial fuel cell operation. Soil, 11(1), 323-338. https://doi.org/10.5194/soil-11-323-2025
24. Negm, N.A., El Hashash, M.A., Abd-Elaal, A., Tawfik, S.M. and Gharieb, A., 2018. Amide type nonionic surfactants: Synthesis and corrosion inhibition evaluation against carbon steel corrosion in acidic medium. Journal of Molecular Liquids, 256, 574-580. http://dx.doi.org/10.1016/j.molliq.2018.02.078
25. Kolbert, C.P. and Persing, D.H., 1999. Ribosomal DNA sequencing as a tool for identification of bacterial pathogens. Current opinion in microbiology, 2(3), 299-305. https://doi.org/10.1016/S1369-5274(99)80052-6
26. Ramírez, S., Torrealba, G., Lameda-Cuicas, E., Molina-Quintero, L., Stefanakis, A.I. and Pire-Sierra, M.C., 2019. Investigation of pilot-scale constructed wetlands treating simulated pre-treated tannery wastewater under tropical climate. Chemosphere, 234, 496-504. https://doi.org/10.1016/J.CHEMOSPHERE.2019.06.081
27. Latkar, M. and Chakrabarti, T., 1994. Performance of upflow anaerobic sludge blanket reactor carrying out biological hydrolysis of urea. Water environment research, 66(1), 12-15. https://doi.org/10.2175/WER.66.1.3
28. Pawlak, Z. and Pawlak, A.S., 1999. Modification of iodometric determination of total and reactive sulfide in environmental samples. *Talanta*, *48*(2), pp.347-353. https://doi.org/10.1016/S0039-9140(98)00253-7
29. Lay, J.J., 2000. Modeling and optimization of anaerobic digested sludge converting starch to hydrogen. Biotechnology and bioengineering, 68(3), 269-278. https://doi.org/10.1002/(SICI)1097-0290(20000505)68:3<269::AID-BIT5>3.0.CO;2-TDigital Object Identifier (DOI)
30. Li, J., Wang, Z., Su, J., Wang, X., Ali, A. and Li, X., 2024. Microbial induced calcium precipitation by Zobellella denitrificans sp. LX16 to simultaneously remove ammonia nitrogen, calcium, and chemical oxygen demand in reverse osmosis concentrates. Environmental Research, 240, 117484. https://doi.org/10.1016/j.envres.2023.117484
31. Li, M., Ali, A., Li, Y., Su, J. and Zhang, S., 2022. The performance and mechanism of simultaneous removal of calcium and heavy metals by Ochrobactrum sp. GMC12 with the chia seed (Salvia hispanica) gum as a synergist. Chemosphere, 297, 134061. https://doi.org/10.1016/j.chemosphere.2022.134061
32. Liu, J., Ali, A., Su, J., Wu, Z., Zhang, R. and Xiong, R., 2021. Simultaneous removal of calcium, fluoride, nickel, and nitrate using microbial induced calcium precipitation in a biological immobilization reactor. Journal of hazardous materials, 416, 125776. https://doi.org/10.1016/j.jhazmat.2021.125776
33. Liu, J., Su, J., Ali, A., Wang, Z. and Zhang, R., 2022a. Potential of a novel facultative anaerobic denitrifying Cupriavidus sp. W12 to remove fluoride and calcium through calcium bioprecipitation. Journal of hazardous materials, 423, 126976. https://doi.org/10.1016/j.jhazmat.2021.126976
34. Liu, J., Su, J., Ali, A., Wang, Z. and Zhang, R., 2022b. Potential of a novel facultative anaerobic denitrifying Cupriavidus sp. W12 to remove fluoride and calcium through calcium bioprecipitation. Journal of hazardous materials, 423, 126976. https://doi.org/10.1016/j.jhazmat.2021.126976
35. Sawalha, H., Alsharabaty, R., Sarsour, S. and Al-Jabari, M., 2019. Wastewater from leather tanning and processing in Palestine: characterization and management aspects. Journal of environmental management, 251, 109596. https://doi.org/10.1016/j.jenvman.2019.109596
36. Wang, Z., Su, J., Ali, A., Gao, Z., Zhang, R., Li, Y. and Yang, W., 2023. Microbially induced calcium precipitation driven by denitrification: performance, metabolites, and

molecular mechanisms. Journal of Environmental Management, 338, 117826. https://doi.org/10.1016/j.jenvman.2023.117826
37. Reyes-Romero, B., Gutiérrez-López, A.N., Hernández-Altamirano, R., Mena-Cervantes, V.Y., Ruiz-Baca, E., Neri-Torres, E.E., Chairez, I., García-Solares, S.M. and Vazquez-Arenas, J., 2021. Removal of concentrated Cr (III) from real tannery wastewater using abiotic and anaerobic processes with native microbial consortia. Journal of Environmental Chemical Engineering, 9(1), 104626. https://doi.org/10.1016/j.jece.2020.104626
38. Sawalha, H., Alsharabaty, R., Sarsour, S. and Al-Jabari, M., 2019. Wastewater from leather tanning and processing in Palestine: characterization and management aspects. Journal of environmental management, 251, 109596. https://doi.org/10.1016/j.jenvman.2019.109596
39. Wang, Z., Su, J., Ali, A., Gao, Z., Zhang, R., Li, Y. and Yang, W., 2023. Microbially induced calcium precipitation driven by denitrification: performance, metabolites, and molecular mechanisms. Journal of Environmental Management, 338, 117826. https://doi.org/10.1016/j.jenvman.2023.117826
40. Varghese, A.P., Neppolian, B. and Lakhera, S.K., 2023. Pitfalls of using nessler's reagent for ammonia detection in photocatalytic nitrogen fixation studies: leveraging 1H NMR for enhanced accuracy and precision. Industrial & Engineering Chemistry Research, 62(32), 12530-12537. https://doi.org/10.1021/acs.iecr.3c01779
41. Subedi, G., Taylor, J., Hatam, I. and Baldwin, S.A., 2017. Simultaneous selenate reduction and denitrification by a consortium of enriched mine site bacteria. Chemosphere, 183, 536-545. https://doi.org/10.1016/j.chemosphere.2017.05.144
42. Wang, Z., Su, J., Ali, A., Gao, Z., Zhang, R., Li, Y. and Yang, W., 2023. Microbially induced calcium precipitation driven by denitrification: performance, metabolites, and molecular mechanisms. Journal of Environmental Management, 338, 117826. https://doi.org/10.1016/j.jenvman.2023.117826
43. Wang, Y., Bai, Y., Su, J., Wang, Z., Li, Y., Gao, Z., Cao, M. and Ren, M., 2024. Kinetic analysis and mechanism of nitrate, calcium, and cadmium removal using the newly isolated Pseudomonas sp. LYF26. Chemosphere, 350, 141156. https://doi.org/10.1016/j.chemosphere.2024.141156
44. Wu, H.Z. and Cao, A., 2013. Preparation and adding methods of Nessler's Reagent having effects on determination of water quality ammonia nitrogen. Advanced Materials Research, 726, 1362-1366. https://doi.org/10.4028/www.scientific.net/AMR.726-731.1362
45. Zhou, L. and Boyd, C.E., 2016. Comparison of Nessler, phenate, salicylate and ion selective electrode procedures for determination of total ammonia nitrogen in aquaculture. Aquaculture, 450, 187-193. https://doi.org/10.1016/j.aquaculture.2015.07.022
46. Wang, Z., Su, J., Ali, A., Zhang, R., Yang, W., Xu, L. and Zhao, T., 2021. Microbially induced calcium precipitation based simultaneous removal of fluoride, nitrate, and calcium by Pseudomonas sp. WZ39: Mechanisms and nucleation pathways. Journal of hazardous materials, 416, 125914. https://doi.org/10.1016/j.jhazmat.2021.125914
47. Wu, H.Z. and Cao, A., 2013. Preparation and adding methods of Nessler's Reagent having effects on determination of water quality ammonia nitrogen. Advanced Materials Research, 726, 1362-1366. https://doi.org/10.4028/www.scientific.net/AMR.726-731.1362
48. Althoff, P.L., 1977. Structural refinements of dolomite and a magnesian calcite and implications for dolomite formation in the marine environment. American

Mineralogist, 62(7-8), 772-783. http://www.minsocam.org/ammin/AM62/AM62_772.pdf

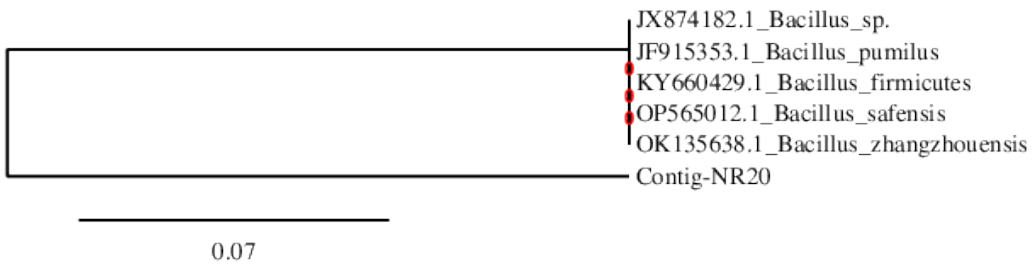


Figure 1. A phylogenetic tree derived from 16S rRNA gene sequence analysis shows the position of strain NR20 among related taxa. The neighbour-joining method was used to construct the tree, and *Bacillus pumilus* was used as the outgroup.

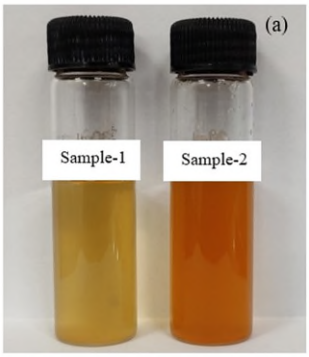


Figure 2. The reduction of nitrate to nitrite by the *Bacillus pumilus* strain. A deep pink colour was produced upon addition of nitrite detection colour reagent.

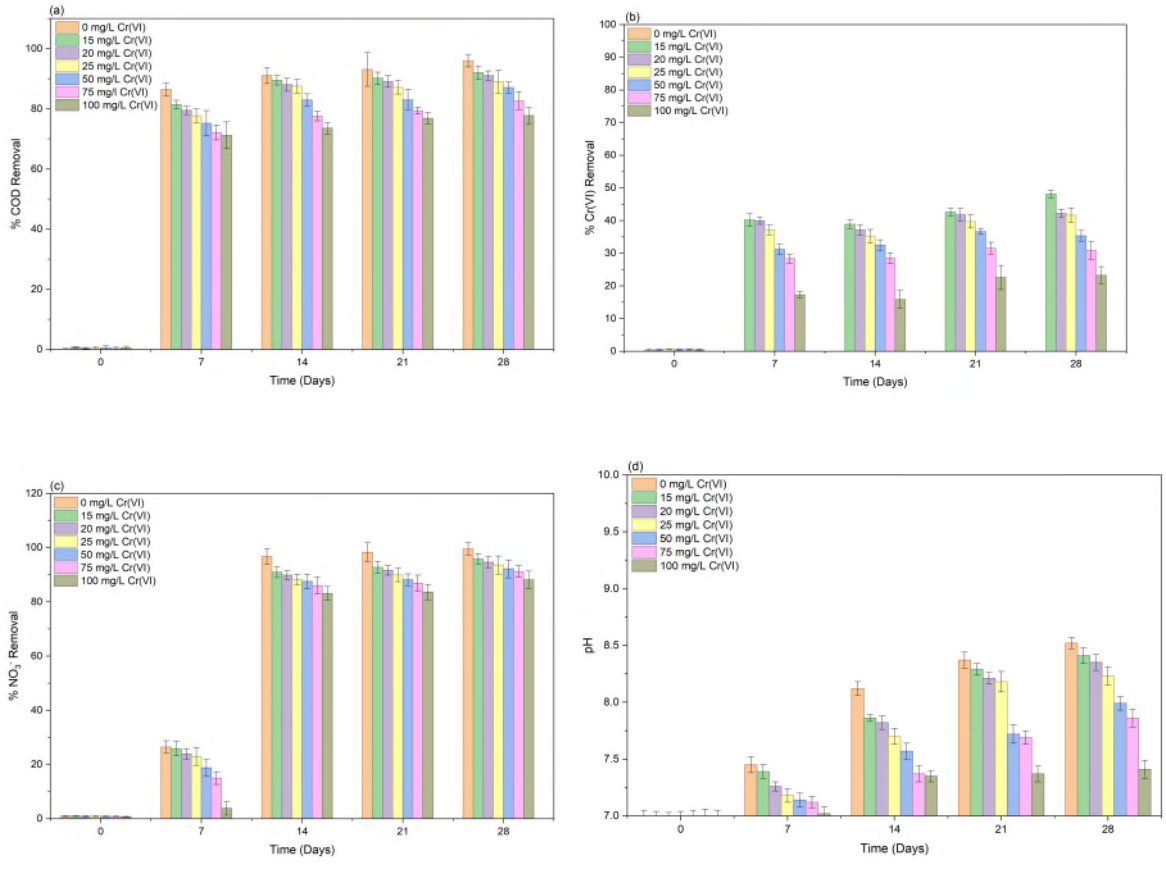
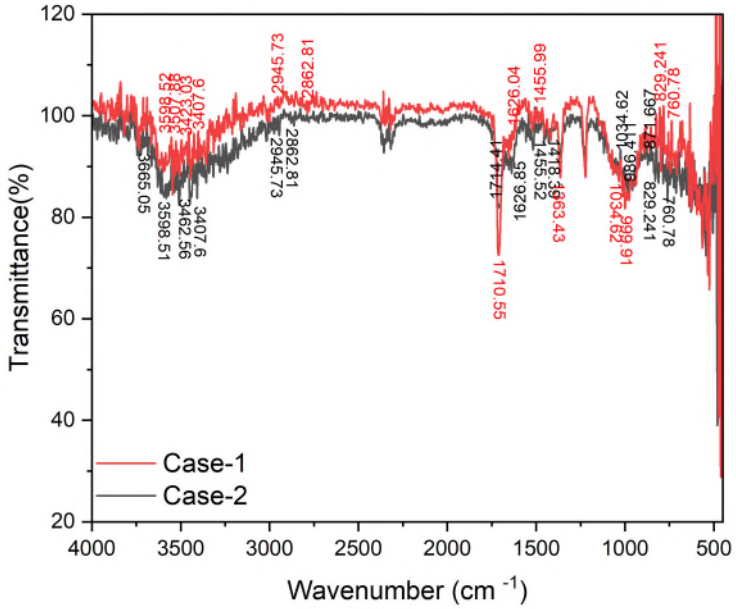


Figure 3. (a) COD removal efficiency, (b) Cr(VI) removal efficiency, (c) Nitrate removal efficiency, (d) pH value

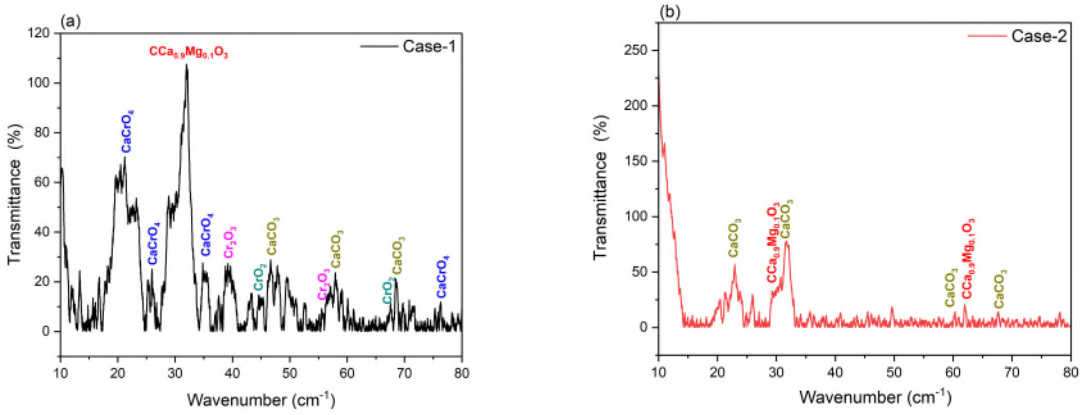


29

30 Figure 4. FT-IR analysis, Case-1: Synthetic tannery wastewater with Cr(VI) concentration, and Case-2: Synthetic tannery
31 wastewater without Cr(VI) concentration.

32

33



34

35 Figure 5. XRD analysis, (a) Case-1: Synthetic tannery wastewater with Cr(VI) concentration, and (b) Case-2: Synthetic tannery
36 wastewater without Cr(VI) concentration.

37

Table 1. COD removal efficiency.

Das	Control	Cr(VI) 15ppm	Cr(VI) 20ppm	Cr(VI) 25ppm	Cr(VI) 50ppm	Cr(VI) 75ppm	Cr(VI) 100ppm
0	0±0.326	0.732±0.196	0.396±0.218	0.327±0.514	0.529±0.628	0.296±0.395	0.518±0.516
7	86.432±2.192	81.395±1.437	79.438±1.376	77.692±2.338	75.185±4.248	72.119±2.476	71.183±4.472
14	91.076±2.706	89.487±1.546	88.013±2.176	87.541±2.236	82.924±2.034	77.574±1.592	73.511±1.886
21	93.048±5.578	90.167±1.998	89.086±1.897	87.109±2.196	83.002±3.432	79.327±1.132	76.831±1.996
28	96.002±2.114	92.043±2.198	91.043±1.543	89.058±3.848	87.063±1.794	82.694±2.946	77.745±2.654

Table 2. Cr(VI) removal efficiency.

Days	Control	Cr(VI) 15ppm	Cr(VI) 20ppm	Cr(VI) 25ppm	Cr(VI) 50ppm	Cr(VI) 75ppm	Cr(VI) 100ppm
0	0	0.236±0.427	0.453±0.147	0.563±0.132	0.471±0.169	0.521±0.182	0.437±0.173
7	0	40.176±1.964	39.954±1.064	37.168±1.514	31.193±1.617	28.356±1.357	17.269±1.072
14	0	38.865±1.265	37.143±1.529	35.269±2.041	32.496±1.641	28.466±1.681	15.844±2.713
21	0	42.564±1.165	41.765±1.993	39.692±1.997	36.653±0.916	31.546±1.846	22.588±3.684
28	0	48.137±1.117	42.186±1.284	41.646±2.251	35.316±1.628	30.864±2.671	23.228±2.671

Table 3. Nitrate removal efficiency.

Days	Control	Cr(VI) 15ppm	Cr(VI) 20ppm	Cr(VI) 25ppm	Cr(VI) 50ppm	Cr(VI) 75ppm	Cr(VI) 100ppm
0	0.913±0.216	0.958±0.158	0.854±0.276	0.892±0.174	0.864±0.151	0.794±0.139	0.726±0.152
7	26.441±2.326	25.865±2.653	23.874±1.976	22.923±3.226	18.774±3.179	14.992±2.317	3.825±2.491
14	95.754±2.917	90.928±1.986	89.847±1.583	88.238±1.962	87.518±2.692	86.016±3.164	83.098±2.584
21	95.893±2.126	92.748±2.196	91.639±1.743	89.932±2.493	88.149±2.197	86.859±2.982	83.606±2.879
28	96.184±2.354	95.794±1.989	94.629±2.145	93.589±3.351	92.182±3.285	91.231±2.173	88.106±3.196

Table 4. pH value.

Days	Control	Cr(VI) 15ppm	Cr(VI) 20ppm	Cr(VI) 25ppm	Cr(VI) 50ppm	Cr(VI) 75ppm	Cr(VI) 100ppm
0	7±0.05	7±0.04	7±0.03	7±0.04	7±0.05	7±0.06	7±0.05
7	7.45±0.07	7.39±0.06	7.26±0.04	7.18±0.06	7.14±0.06	7.12±0.05	7.02±0.06
14	8.12±0.06	7.86±0.03	7.82±0.06	7.7±0.07	7.57±0.07	7.37±0.07	7.35±0.05
21	8.37±0.07	8.29±0.05	8.21±0.05	8.18±0.09	7.72±0.08	7.69±0.06	7.37±0.07
28	8.52±0.05	8.41±0.07	8.35±0.07	8.23±0.08	7.99±0.06	7.86±0.08	7.41±0.08